ELSEVIER

Thin Solid Films 322 (1998) 213–217

thin solid films

Properties of thin Ta–N films reactively sputtered on $Cu/SiO_2/Si$ substrates

Jui-Chang Chuang *, Mao-Chieh Chen

Department of Electronics Engineering and the Institute of Electronics, National Chiao-Tung University, 1001 Ta Hsueh Road, Hsinchu, 300, Taiwan

Received 29 July 1997; accepted 23 October 1997

Abstract

This work studied the thin film properties of 200 Å Ta and Ta–N films reactively sputtered on the $Cu/SiO_2/Si$ substrates. The nitrogen atomic concentration in the Ta–N film was found to saturate at about 30%. Excessive sputtering gas flow, especially the N_2 gas, caused surface damage to the sputter deposited films. Thermal annealing in N_2 ambient at temperatures up to 700°C did not change the atomic concentrations and the chemical states of Ta and N in the Ta and Ta–N films. The thermal annealing resulted in the grain growth and the healing of sputter damage, but it also induced new defects in the Ta–N films due to thermal stress. This presents a reliability problem in process application involving high temperature thermal cycle.

Keywords: Thin film properties; Ta–N; $Cu/SiO_2/Si$

1. Introduction

Tantalum (Ta) and Tantalum nitrides (Ta–N) have been used as diffusion barriers in copper (Cu) metallization against interaction between Cu and the underlying substrates [1–5], and they have been recognized as excellent barriers for the prevention of Cu-diffusion. The damascene scheme of Cu chemical–mechanical polishing (CMP) process uses Ta liners to passivate the interlaced Cu layers [6]. Ta and Ta–N are attractive in many applications because of their good electrical conductivity, high melting point, and chemical inertness [7–9]. They belong to the class of dense interstitial compound [2] and are expected to be low reactive with Cu. Many methods have been reported for the deposition of Ta and Ta–N films, for example, reactive sputtering [2–5,10], ion beam assisted deposition (IBAD) [11], and E-beam evaporation [12–15] of Ta–N on silicon [2–5,10–15], carbon [10], stainless steel [11], and silicide [13,14] substrates. In this work, we investigated the thin film properties of 200 Å Ta and Ta–N films reactively sputtered on Cu substrate. This is the beginning phase of study for the passivation capability of Ta and Ta–N films against Cu oxidation in the $Ta/Cu/SiO_2/Si$ and $Ta–N/Cu/SiO_2/Si$ structures.

2. Experimental details

The substrates used for the deposition of Ta and Ta–N films were p-type, boron-doped Si wafers with nominal resistivity of 17–55 Ω cm. After initial RCA cleaning, the Si wafers were thermally oxidized at 1050°C in steam atmosphere to grow a 5000 Å SiO_2. A Cu film of 2000 Å thickness was sputter deposited on the oxide layer. This was followed by a 200 Å Ta or Ta–N film deposition on the Cu layer. The Ta film was sputter deposited using a pure Ta target in Ar ambient, while the Ta–N films were deposited by reactive sputtering using the same Ta target in a gas mixture of Ar and N_2 with various flow rates. The base pressure of the sputtering chamber was 5×10^{-7} Torr, and films were sputtered at a pressure of 7.8 mTorr. Table 1 summarizes the sputtering conditions for the Ta and Ta–N films. After the film deposition, wafers were diced into 1.5×1.5 cm^2 pieces for further treatment. The diced samples were thermally annealed in flowing N_2 for 30 min at a temperature ranging from 100 to 700°C. Electrical measurement and material analysis were used to study the film properties. Sheet resistance was measured using a 4-point probe. Scanning electron microscope (SEM)

* Corresponding author.

0040-6090/98/$19.00

Table 1
Sputtering conditions for Ta and Ta–N films

Sample identification	A	B	C	D	E
Ar/N_2 flow rates (sccm)	(12/0)	(58.5/1.5)	(12/3)	(12/5)	(12/12)
Volume fraction of N_2 in sputtering gas (%)	0	2.5	20	29	50
Deposition rate (Å/s)	0.3	0.45	0.3	0.3	0.17

was used to investigate surface morphology. Auger electron spectroscopy (AES) was used for depth profile analysis. X-ray photoelectron spectroscopy (XPS) was used for chemical states analysis.

3. Results and discussion

Fig. 1 shows the atomic concentrations (at.%) of nitrogen in the sputter deposited films vs. N_2 volume fraction in the sputtering gas, as determined from the AES analysis. No nitrogen was detected for samples A and B. The nitrogen at.% was found to be 23.5% for sample C, and increased to 30.5% for sample D. However, no further increase of nitrogen at.% was found for sample E, which was deposited in an Ar/N_2 gas mixture with 50% volume fraction of N_2. The nitrogen at.% in Ta–N saturated at about 30%. The chemical states of tantalum and nitrogen in these films were determined using XPS under Mg–K α X-ray irradiation by taking C1s (285 eV) and Cu 2p (932.7 eV) as energy references. Fig. 2 shows the binding energy spectra of Ta $4f_{7/2}$ and N1s photoelectrons. For sample A and sample B, the binding energy of Ta $4f_{7/2}$ photoelectrons was determined to be 22.8 eV, while no nitrogen signal was found. For the N-doped sample C and sample D, the binding energy of Ta $4f_{7/2}$ photoelectrons shifted to 23.5 eV, and N1s signal was found at 398.2 eV. The binding energies of Ta $4f_{7/2}$ photoelectrons of stoichiometric bcc Ta and fcc Ta–N compounds are 21.9 [16] and 22.6 [11] eV, respectively. It was reported that the Ta film sputter deposited in Ar ambient belonged to tetragonal Ta, while the reactively sputtered Ta–N film belonged to

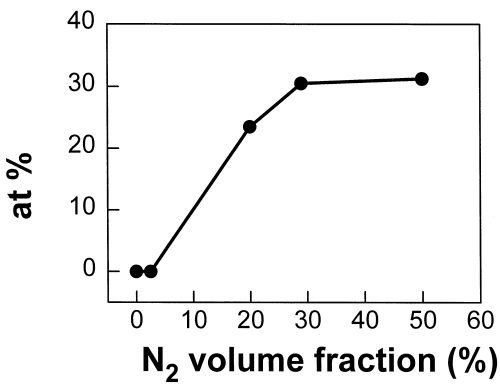

Fig. 1. Atomic concentrations (at.%) of nitrogen in sputter deposited Ta and Ta–N films vs. N_2 volume fraction in the sputtering gas.

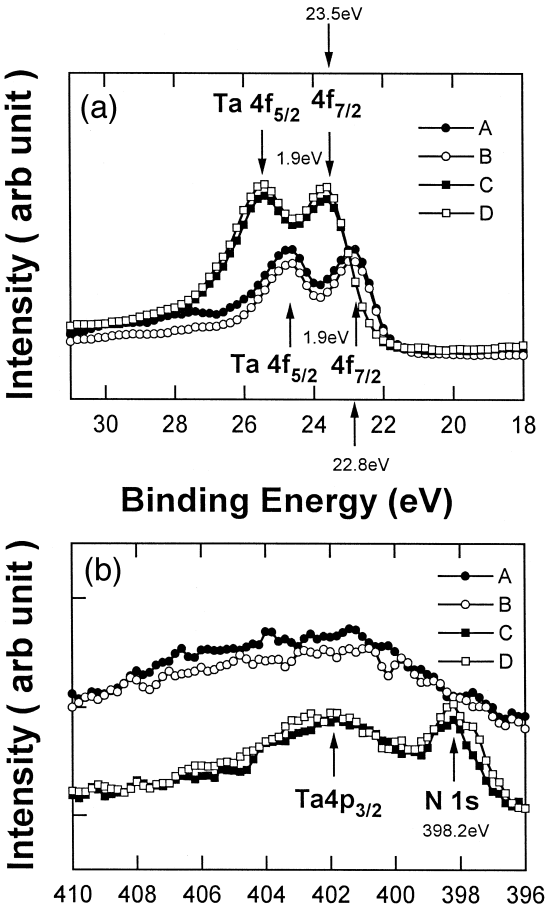

Fig. 2. XPS spectra of (a) Ta $4f_{7/2}$ and (b) N1s photoelectrons for the Ta and Ta–N films (samples A, B, C, and D).

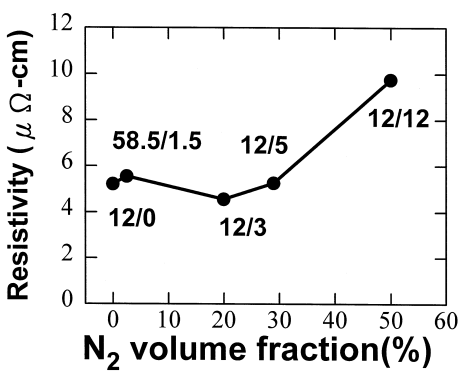

Fig. 3. Resistivity of the as-deposited Ta and Ta–N films vs. N_2 volume fraction in the sputtering gas mixture (Ar/N_2). The gas flow rates (Ar/N_2, in unit of sccm) are indicated for each sample.

either hexagonal TaN or hexagonal Ta_2N structure [17]. The discrepancy in binding energies of the Ta $4f_{7/2}$ photoelectrons is presumably due to structure difference.

The resistivity and the surface morphology of the as-deposited films are shown in Figs. 3 and 4, respectively. It can be seen that the film resistivity, surface morphology, and sputtering gas mixture are closely related. Comparison between samples A and B shows that high Ar flow rate in the sputtering gas resulted in higher sputtering rate and cracked surface (Fig. 4b); thus sample B is slightly more resistive than sample A. Samples C and D were deposited in Ar/N_2 gas mixture with the same flow rate of Ar but different flow rate of N_2. They had the same sputtering rate, but the higher N_2 content in the sputtering gas

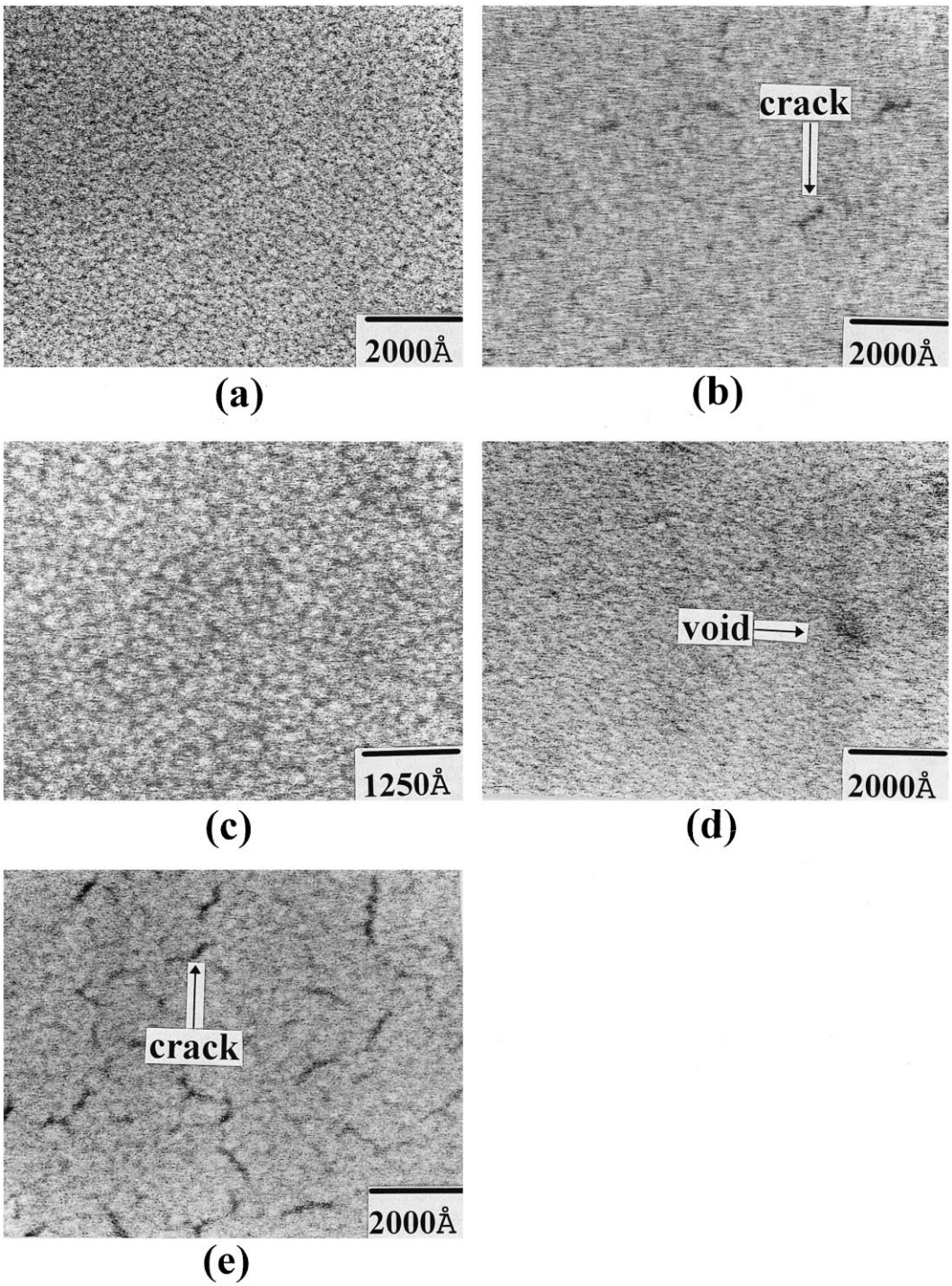

Fig. 4. SEM micrographs showing surface morphology of the as-deposited Ta and Ta–N films: (a) sample A, (b) sample B, (c) sample C, (d) sample D, and (e) sample E.

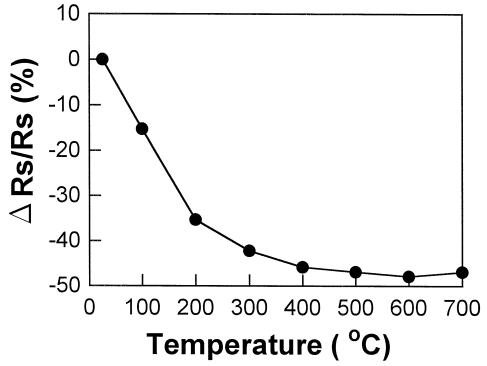

Fig. 5. Sheet resistance change vs. N_2 annealing temperature for sample C.

resulted in voided surface (Fig. 4d) and higher resistivity of sample D. As the N_2 volume fraction increased further for the deposition of sample E, the sputtering rate dramatically reduced and the surface became seriously damaged (Fig. 4e); thus, sample E has a much higher resistivity.

In the sputtering process, sputter deposition and sputter etching occur simultaneously [18]. Both energetic Ar and N_2 plasma contributed to the sputter deposition and to the sputter etching. By keeping the same deposition pressure, i.e., 7.8 mTorr, for all the samples deposited, we assume that large Ar flow caused surface damage of sample B (Fig. 4b). Nitrogen in the sputtering gas mixture not only introduced nitrogen into Ta films but also caused excessive energetic nitrogen particles to impinge upon the deposited Ta–N surface. With more than 30% volume fraction of N_2 in the sputtering gas (sample E), sputter etching took predominance, resulting in decrease of Ta–N deposition rate and saturation of nitrogen at.% in the deposited Ta–N films (Fig. 1). The similar trend in the saturation of nitrogen content was reported [10]. We assume that the sputter etching due to excessive energetic N_2 plasma in the sputtering gas mixture was responsible for the nitrogen at.% saturation in the deposited Ta–N films. In addition, the impinging energetic N_2 plasma also caused surface damage as shown in Fig. 4e.

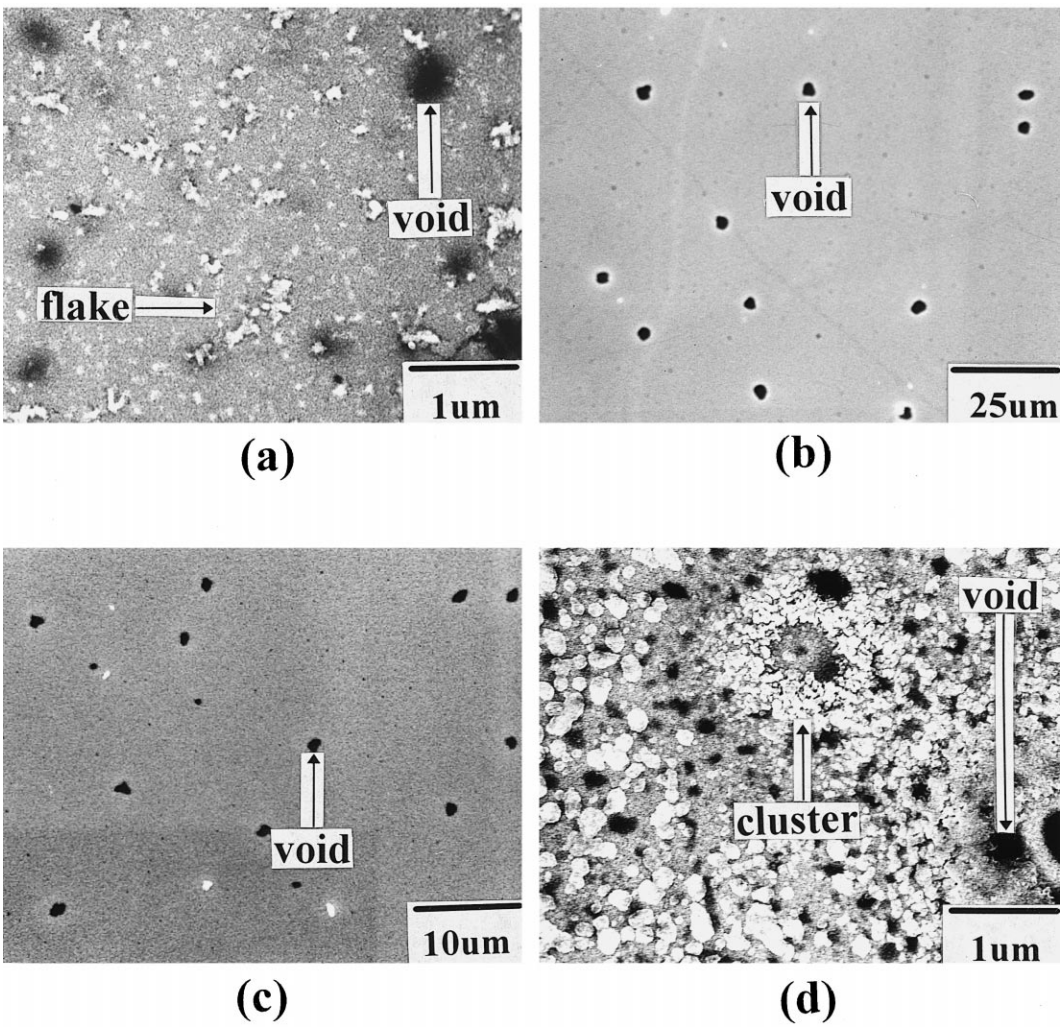

Fig. 6. SEM micrographs showing surface morphology of Ta and Ta–N films for the samples thermally annealed at 700°C in N_2 ambient: (a) sample A, (b) sample C, (c) sample D, and (d) sample E.

Fig. 5 shows the sheet resistance change vs. annealing temperature for the thermally N_2 annealed sample C. The similar trend showing decreasing sheet resistance with increasing annealing temperature was obtained for the other samples. The reduction of sheet resistance was presumably due to grain growth and sputter damage healing of the Ta–N film by thermal annealing. Fig. 6 shows the surface morphology of Ta–N films after the Ta–N/Cu/SiO_2/Si structure was thermally annealed at 700°C in N_2 ambient. Compared to the as-deposited films shown in Fig. 4, new defects were found on the surface of the thermally annealed samples; these include voids for all thermally stressed samples, flaking due to agglomeration of Ta grains for sample A (Fig. 6a), and cluster observed on sample E (Fig. 6d). Surface morphology of sample B looks the same as that of sample A. Film stress may be created because of accommodating of thin Ta or Ta–N film's surface tension during the thermal heating and cooling contours and the difference of grain growth rates between the films and the underlying Cu layers [18]. To relieve this thermal stress, voids were formed, as shown in Fig. 6. The cluster on sample E was presumed to be a kind of copper oxide cluster, because there was residual oxygen in the annealing ambient and the surface of the as-deposited sample E was seriously damaged (Fig. 4e).

The thermal annealing did not result in detectable change of nitrogen at.% in the Ta–N films and chemical states of Ta and N in the Ta and Ta–N films. The binding energies of the Ta $4f_{7/2}$ and N1s photoelectrons remained the same as those shown in Fig. 2. Moreover, the elemental depth profiles for the 700°C annealed sample C and sample D, as determined by AES and XPS analysis, showed negligible change as compared to those of the as-deposited sample C and sample D, respectively. This implies that there was negligible interaction between Cu and Ta as well as Cu and Ta–N. Nevertheless, the thermal stress degraded surface morphology of the Ta and Ta–N layers.

4. Conclusions

Sputtered Ta and reactively sputtered Ta–N films deposited on Cu/SiO_2/Si substrates were studied. High flow rate of Ar sputtering gas led to faster sputtering rate as well as cracked Ta films. Moreover, high flow rate of N_2 in the sputtering gas mixture introduced excessive energetic N_2 plasma, resulting in reduced deposition rate as well as damaged and higher resistive Ta–N films. The nitrogen atomic concentration in the Ta–N film saturated at about 30%. We assume that the saturation of nitrogen at.% in the Ta–N film is a consequence of sputter etching due to excessive energetic N_2 plasma. The nitrogen at.% and the chemical states of Ta and N for all samples did not change after thermal annealing at temperatures up to 700°C in N_2 ambient. Thermal annealing of the Ta–N/Cu/SiO_2/Si structures resulted in reduced sheet resistance due to grain growth and sputter damage healing of the films; however, new defects were created due to the thermal stress, presenting a reliability problem in process application.

Acknowledgements

The authors wish to thank the Semiconductor Research Center of National Chiao-Tung University and the National Nano Device Laboratory for providing excellent processing environment. This work was supported by the National Science Council, ROC, under Contract No. NSC-86-2215-E-009-040.

References

[1] S.Q. Wang, S. Suthar, C. Hoeflich, B.J. Burrow, J. Appl. Phys. 73 (5) (1993) 2301.
[2] K. Holloway, P.M. Fryer, C. Cabral Jr., J.M.E. Harper, P.J. Bailey, K.H. Kelleher, J. Appl. Phys. 71 (11) (1992) 5433.
[3] T. Nakano, H. Ono, T. Ohta, T. Oku, M. Murakami, in: Proceeding of 1994 VMIC Conference, 1994, p. 407.
[4] M. Stavrev, C. Wenzel, A. Möller, K. Drescher, Appl. Surf. Sci. 91 (1995) 257.
[5] B. Mehrotra, J. Stimmell, J. Vac. Sci. Technol. B5 (6) (1987) 1736.
[6] C.-K. Hu, B. Luther, F.B. Kaufman, J. Hummel, C. Uzoh, D.J. Pearson, Thin Solid Films 262 (1995) 84.
[7] D.R. Lide (Ed.), CRC Handbook of Chemistry and Physics, 73rd edn., CRC Press, Boca Raton, 1992.
[8] E.A. Brandes (Ed.), Smithells Metals Handbook, 6th edn., Butterworths, Borough Green, Sevenoaks, England, 1983.
[9] T.B. Massalski (Ed.), Binary Phase Diagram, 2nd edn., ASM International, Material Park, OH, 1990.
[10] X. Sun, E. Kolawa, J.-S. Chen, J.S. Reid, M.-A. Nicolet, Thin Solid Films 236 (1993) 347.
[11] K. Baba, R. Hatada, Surf. Coat. Technol. 84 (1996) 429.
[12] L.A. Clevenger, N.A. Bojarczuk, K. Holloway, J.M.E. Harper, C. Cabral Jr., R.G. Schad, F. Cardone, L. Stolt, J. Appl. Phys. 73 (1) (1993) 300.
[13] C.-A. Chang, J. Appl. Phys. 67 (12) (1990) 7348.
[14] C.-A. Chang, J. Vac. Sci. Technol. A8 (5) (1990) 3796.
[15] W. Ensinger, M. Kiuchi, M. Satou, J. Appl. Phys. 77 (12) (1995) 6630.
[16] C.D. Wagner, W.M. Riggs, L.E. Davis, J.F. Moulder, in: G.E. Muilenberg (Ed.), Handbook of X-ray Photoelectron Spectroscopy, Perkin-Elmer, Physical Electronics Division, Eden Prairie, MN, 1979.
[17] D.D. Wu, Master Thesis, National Chiao-Tung University, Taiwan, 1996.
[18] S.P. Murarka, in: S.M. Sze (Ed.), VLSI Technology, 2nd edn., Chap. 9, McGraw-Hill, Singapore, 1988.